Journal of Materials Chemistry A

ROYAL SOCIETY OF CHEMISTRY

PAPER

View Article Online
View Journal

Cite this: DOI: 10.1039/d0ta04734a

High-efficiency organic solar cells enabled by halogenation of polymers based on 2D conjugated benzobis(thiazole)†

Shuguang Wen, [ab] Yonghai Li, [ab] Nan Zheng,[c] Ibrahim Oladayo Raji, [a] Chunpeng Yang[a] and Xichang Bao*[ab]

With the rapid development of non-fullerene acceptors, polymer donor design is critical for the realization of significantly higher power conversion efficiencies in organic solar cells (OSCs). The donor–acceptor (D–A) alternating structure is an effective strategy for the design of polymers due to its advantages in optical absorption, energy level modulation, charge mobilities, *etc.* Nevertheless, the current development of polymers is restricted in terms of modification of the acceptor unit. In this work, a 2D conjugated acceptor unit of benzobis(thiazole) was designed for constructing wide bandgap polymers. Fluorine and chlorine atoms were introduced into the polymers to modulate the energy levels and film morphology. The photovoltaic performances of the polymers were examined by fabricating devices employing IT-4F as the acceptor. All three polymers exhibit high short-circuit densities (J_{SC}s) of over 21 mA cm^{-2} in the devices which could be attributed to high extinction coefficient and beneficial face-on orientation, as featured by the polymers based on the 2D conjugated BBT unit. Incorporation of F- or Cl-atoms effectively improved all three photovoltaic parameters open-circuit voltage (V_{OC}), J_{SC} and fill factor. As a result, a high power conversion efficiency of 14.8% was achieved for the chlorinated polymer (PBB-Cl). A high V_{OC} of 0.94 V and J_{SC} of 21.8 mA cm^{-2} were realized in the devices, indicating well-balanced V_{OC} and J_{SC} values. Dominant face-on orientation was observed for all three polymer films, which is beneficial for charge transport in the vertical direction of the substrate. Given the excellent photovoltaic performance achieved in the devices, the polymer based on the 2D conjugated BBT unit would be a very promising candidate for high performance organic solar cells.

Received 7th May 2020
Accepted 19th June 2020

DOI: 10.1039/d0ta04734a

rsc.li/materials-a

Introduction

Organic solar cells (OSCs) have attracted much attention due to their flexibility, light weight, low-cost mass production, and potential application in portable electronic devices.[1–6] With the efforts on the exploration of efficient light-harvesting materials,[6–14] interfacial materials,[15–20] and device engineering,[21–23] photovoltaic parameters are substantially optimized and high power conversion efficiencies (PCEs) of over 15% have been achieved.[6,24–27] Nevertheless, the efficiencies of OSCs still lag behind those of inorganic solar cells and perovskite solar cells. Unlike that of inorganic solar cells, the active layer of OSCs usually adopts a bulk heterojunction (BHJ) structure comprising a blend of donor and acceptor materials. Excitons are generated first in donor or acceptor materials and then separated into free carriers at the interface. Energy level offset is usually necessary for achieving efficient exciton dissociation, but induces large energy loss (E_{loss}),[28,29] which is one of the main factors impeding the development of OSCs. Therefore, it is pertinent to adjust the energy levels of donor and acceptor materials carefully.

Complementary optical absorption with low bandgap small molecule acceptors and wide bandgap donors is a constructive strategy for achieving high-efficiency non-fullerene OSCs (NF-OSCs). In this system, the acceptor determines the upper limit of open circuit voltage (V_{OC}) and short circuit density (J_{SC}), thus generally determining the overall photovoltaic efficiency. Various acceptors have been explored and their efficiencies have accordingly been greatly improved during the past few years.[30] Meanwhile, donor materials are critical for achieving maximum efficiency. Donor–acceptor (D–A) type organic semiconductors usually exhibit a narrow width absorption peak, so donor materials with complementary optical absorption can maximize the utilization of light and achieve a high J_{SC} value. In addition, matching energy levels and good miscibility between donor/

[a]CAS Key Laboratory of Bio-based Materials, Qingdao Institute of Bioenergy and Bioprocess Technology, Chinese Academy of Sciences, Qingdao 266101, China. E-mail: baoxc@qibebt.ac.cn

[b]Functional Laboratory of Solar Energy, Shandong Institute of Energy, Qingdao 266101, China

[c]State Key Laboratory of Luminescent Materials and Devices, South China University of Technology, Guangzhou 510640, China

†Electronic supplementary information (ESI) available. See DOI: 10.1039/d0ta04734a

acceptor materials are vital for exciton dissociation and charge transport. Therefore, rational design of the donor material is important to obtain optimum efficiency. Introduction of halogen atoms is an important and propitious strategy in polymer donor design.[31–36] It can reduce the molecular energy levels due to electronegativity, thus achieving high V_{OC} in photovoltaic devices or reasonable energy level alignment between the donor and the acceptor. Furthermore, halogen atoms can also influence molecular interaction by the formation of non-covalent bonds to obtain an appealing film morphology. Consequently, materials containing halogen atoms usually exhibit excellent photovoltaic performance.[37,38]

Benzo[1,2-*d*:4,5-*d*′]bis(thiazole) (BBT) is a weak electron withdrawing building block for organic semiconductors.[39] Its attractive and impressive feature is that it has immense potential for structural modification which is different from other existing building blocks such as 1,3-bis(4-(2-ethylhexyl) thiophen-2-yl)-5,7-bis(2-alkyl)benzo[1,2-*c*:4,5-*c*′]dithiophene-4,8-dione (BDD), benzotriazole (BTA), and 2,1,3-benzothiadiazole (BT). This would open up a new approach for modulating energy levels and molecular packing of materials. The BBT unit has been applied in the construction of conjugated copolymers for organic opto-electronic devices such as organic field-effect transistors[40] and organic solar cells.[41] These types of copolymers show good hole mobility and excellent durability making them worthy to be considered for practical applications. Previously, we have reported a BBT-based copolymer PBB-T and applied it in non-fullerene organic solar cells.[42] The polymer showed a wide optical band gap of 2.10 eV and an intense photo response in the wavelength range between 430 and 570 nm. A high PCE of 13.3% was achieved in OSC devices. In the molecular structure of PBB-T, branched side chains are introduced into its thiophene spacers to guarantee solubility, but they affect backbone planarity and hence, reduce the ordered molecular packing and charge mobility.

In this study, we introduced alkylthiophene side chains at the 4,8-positions of the BBT unit to construct a 2D conjugated acceptor building block. Three conjugated polymers (PBB-H, PBB-F, and PBB-Cl) were synthesized by copolymerization of BBT and benzo[1,2-*b*:4,5-*b*′]dithiophene (BDT) monomers (Fig. 1). Thus fully conjugated polymers were constructed, which would be beneficial for absorption coefficient and light harvesting of the polymers.[43] Fluorine and chlorine atoms were introduced into the BDT unit to optimize the energy levels and film morphology. The photovoltaic performances of these polymers were evaluated with IT-4F as the acceptor. It was observed that all three polymers showed excellent J_{SC} values of over 21 mA cm^{-2} in the devices. The encouraging J_{SC} values could be probably contributed by their high extinction coefficients and favorable face-on orientation. High PCEs of 14.7% and 14.8% were achieved for PBB-F and PBB-Cl, respectively, which are much higher than that of PBB-H (12.0%). All three photovoltaic parameters J_{SC}, V_{OC} and FF are simultaneously increased, indicating the effectiveness of halogenation in the design of photovoltaic materials. A high V_{OC} of 0.94 V is achieved for PBB-Cl with an E_{loss} of 0.60 eV, which is one of the best values for IT-4F based devices. The J_{SC} and V_{OC} values are well-balanced by the halogenation of these BBT-based polymers. These results indicate that the polymers based on 2D conjugated BBT would be excellent donor materials for high-efficiency OSCs.

Results and discussion

Materials synthesis and characterization

Fig. 1 shows the synthesis routes of the BBT-based polymers. The key 2D conjugated BBT intermediate 1 was synthesized according to the literature.[44] Two flanking thiophenes were then introduced by the Stille reaction and the bromide monomer 3 was obtained by using *n*-BuLi/CBr_4. With the monomer in hand, polymers PBB-H, PBB-F and PBB-Cl were synthesized by Pd-catalyzed Stille coupling reaction with three types of benzodithiophene monomers (BDT-X), respectively. All of these polymers are readily soluble in chlorobenzene at room temperature,

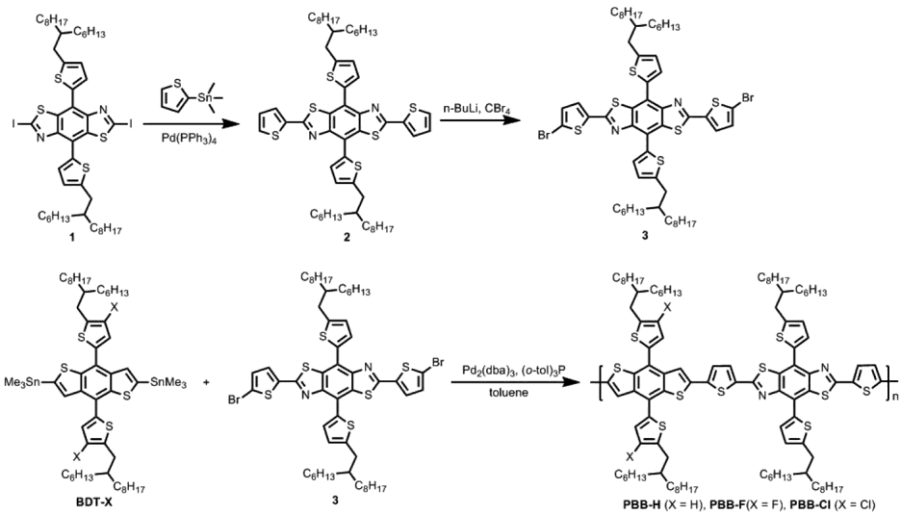

Fig. 1 Chemical structures and synthesis routes of PBB-H, PBB-F and PBB-Cl.

which allows the devices to be processed by a simple spin-coating approach. The number-average molecular weight (M_n) was determined to be 146.9, 34.9 and 76.8 kDa with a PDI of 2.15, 2.23 and 2.37 by high temperature gel permeation chromatography (GPC) analysis for PBB-H, PBB-F, and PBB-Cl, respectively. The decomposition temperatures (T_d, 5% weight loss) were measured by thermogravimetric analysis (TGA) under a nitrogen atmosphere to be 426 °C (PBB-H), 435 °C (PBB-F) and 434 °C (PBB-Cl), indicating enough thermal stability for solar cell fabrication (Fig. S1†).

Optical properties and energy levels

The optical absorption pro珋les of the polymers are shown in Fig. 2. These polymers show obvious shoulder peaks at about 571 nm in dilute chlorobenzene solution, indicating strong aggregation behaviors. The absorption pro珋les of these polymers as thin 珋lms are similar to each other due to the same conjugated backbone. Two main peaks are located at a wavelength of about 535 and 579 nm with an optical bandgap of 2.0 eV, red-shi沢ed by about 25 nm compared to that of 1D BBT-based polymer PBB-T.[42] This difference can be ascribed to the extension of p-conjugation and enhanced p–p interaction.[45] The extinction coefficients (3_{max}) of PBB-H, PBB-F and PBB-Cl were determined to be 1.53×10^5 (572 nm), 1.39×10^5 (530 nm) and 1.27×10^5 (528 nm) $M^{-1}\,cm^{-1}$ in solution and 8.3×10^4, 8.2×10^4 and 7.4×10^4 cm^{-1} at rv580 nm for neat 珋lms, respectively. High extinction coefficient values would facilitate light harvesting in thin 珋lms (rv100 nm), which is bene珋cial for efficient charge extraction while avoiding charge recombination.[46]

The molecular geometries and electronic properties of the polymers were investigated by density functional theory (DFT) simulations using Gaussian 09 at the B3LYP/6-31G(d,p) level. To simplify the calculation, two repeating units of the polymer were used and the alkyl side chains were replaced by methyl groups (Fig. S2†). Impressively, the HOMO electron cloud is more delocalized over the thiophene beside BBT than that beside BDT, which is probably induced by the smaller dihedral angle between thiophene and BBT (rv37°) than that between thiophene and BDT (rv52°). The delocalization (conjugate effect) can induce a red shi沢 of the absorption spectra, which is in accordance with the red-shi沢ed absorption of these designed polymers. The HOMO/LUMO energy levels were calculated to be —4.95/2.50, —5.04/—2.59 and —5.07/—2.62 eV for PBB-H, PBB-F, and PBB-Cl, respectively. It is shown that the HOMO energy levels are gradually reduced with the introduction of F and Cl atoms. Then, the energy levels of the polymers were also obtained by electrochemical cyclic voltammetry (CV) experiments and the results are summarized in Table 1. The HOMO/LUMO energy levels were estimated to be —5.47/—3.47, —5.57/—3.57 and —5.64/—3.64 eV, respectively for PBB-H, PBB-F, and PBB-Cl (Fig. S3†). Similar to the calculated results, the HOMO energy levels are gradually decreased and approach the value of IT-4F (—5.70 eV), and thus the energy loss would be effectively reduced in OSCs. Therefore, V_{OC} is expected to gradually increase in OSC devices, which would facilitate the modulation of the balance between J_{SC} and V_{OC} values.

Photovoltaic properties

The photovoltaic performance of the polymers was evaluated with the device structure of glass/ITO (indium tin oxide)/PEDOT:PSS (poly(3,4-ethylenedioxythiophene):poly(styrenesulfonate))/active layer/PDINO (perylene diimide functionalized with amino *N*-

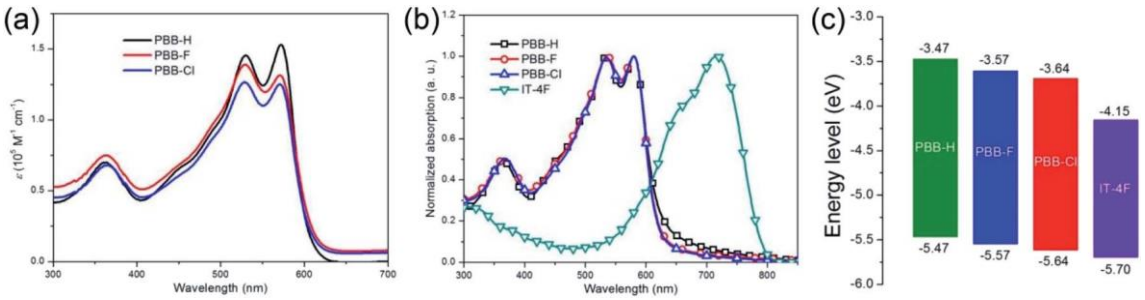

Fig. 2 (a) UV-vis absorption spectra of the polymers in dilute chlorobenzene; (b) normalized UV-vis absorption spectra of thin films; and (c) energy level diagrams of PBB-H, PBB-F, PBB-Cl and IT-4F.

Table 1 Optical and electrochemical properties of the polymers

Polymer	l_{max} [nm] Solution	Film	E_g^{opt} [eV]	3_{max} [a] [$10^5 M^{-1} cm^{-1}$]	E_{HOMO} [b] [eV]	E_{LUMO} [c] [eV]
PBB-H	572	580	2.0	1.53	—5.47	—3.47
PBB-F	529	579	2.0	1.39	—5.57	—3.57
PBB-Cl	528	580	2.0	1.27	—5.64	—3.64

[a] Measured in dilute chlorobenzene solution. [b] Measured by cyclic voltammetry measurement. [c] Calculated from $E_{LUMO} = E_{HOMO} + E_g^{opt}$.

oxide[47])/Al. IT-4F was used as the acceptor material combined with BBT-based polymers as active layers. Fig. 3 shows the current density–voltage (*J*–*V*) curves of the optimized devices with a donor/acceptor weight ratio of 1 : 1 and the photovoltaic parameters are summarized in Table 2. The detailed device fabrication procedure is presented in the ESI (Tables S1–S3†). The best performances were achieved with the combination of thermal annealing and diphenyl ether (DPE) treatment through the device optimization process. Under the optimized conditions, the device based on PBB-H:IT-4F shows a good efficiency of 12.0% with a V_{OC} of 0.85 V, a J_{SC} of 21.5 mA cm^{-2} and a 珡ll factor (FF) of 65.6%. With the introduction of 珞uorine atoms, the device based on PBB-F:IT-4F exhibits an impressive PCE of 14.7% with a V_{OC} of 0.92 V, a J_{SC} of 22.4 mA cm^{-2} and a FF of 71.1%. All the device parameters are simultaneously improved, indicating that 珞uorination is an effective approach for improving photovoltaic performance. As for the chloride polymer PBB-Cl, the related device shows the highest PCE of 14.8% with a V_{OC} of 0.94 V, a J_{SC} of 21.8 mA cm^{-2} and a FF of 72.5%. The V_{OC} values for PBB-H, PBB-F, and PBB-Cl are 0.85, 0.92 and 0.94 V, thus affording an E_{loss} of 0.69, 0.62 and 0.60 eV, respectively, which conform with their gradually decreasing HOMO energy levels. The E_{loss} of 0.60 eV achieved for the PBB-Cl:IT-4F based device is one of the lowest values for the device with IT-4F as the acceptor (Table S4†).[9,33,48,49] All three polymers show similar J_{SC} values of over 21 mA cm^{-2} in the devices due to the similar narrow bandgap acceptor employed. The high J_{SC} values achieved would be related to the high extinction coefficient of the polymers based on 2D conjugated BBT. With the introduction of halogen atoms, the FF values of the devices based on PBB-F (71.1%) and PBB-Cl (72.5%) are effectively improved than that of PBB-H (65.6%). It is known that the introduction of halogen atoms can not only modulate the energy levels but also effectively regulate the aggregation characteristics of the materials. Therefore, the increase of FF values is probably induced by the more bene珞cial 珞lm morphology (*vide infra*). Ultimately, a high efficiency of 14.8% is achieved for the devices based on PBB-Cl:IT-4F, which is the highest value for non-fullerene OSCs with IT-4F as the acceptor (Fig. S4†). Furthermore, another batch of PBB-H and PBB-Cl was synthesized with a M_n/PDI of 48.5 kDa/2.35 and 48.9 kDa/2.23, respectively, which are similar to that of PBB-F (35 kDa/2.23). The PCEs were measured to be 11.8% and 14.6% for PBB-H:IT-4F and PBB-Cl:IT-4F, respectively, demonstrating that the efficiencies are almost not affected by the variation of molecular weight (Fig. S5†). These results also verify the good reproducibility of the performance for these polymers.

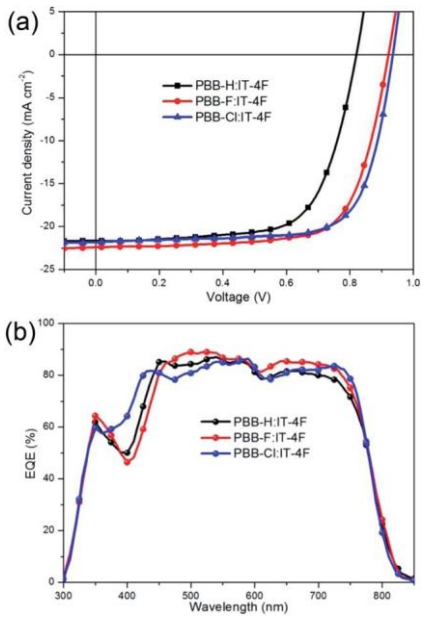

Fig. 3 (a) *J*–*V* curves and (b) the corresponding EQE spectra of the OSCs based on polymer:IT-4F.

Fig. 3b shows the external quantum efficiency (EQE) curves of the optimal polymer:IT-4F devices. All the devices exhibit a good photo response in the wavelength region of 400 to 800 nm. The current density values obtained from the EQE spectra are 20.9, 21.4 and 21.1 mA cm^{-2} for PBB-H:IT-4F, PBB-F:IT-4F and PBB-Cl:IT-4F respectively, which are consistent with the J_{SC} values from the *J*–*V* curves and con珞rm the reliability of the results. As known from the optical absorption spectra, the short wavelength region below 620 nm is contributed primarily by the polymer and the long wavelength region above 620 nm is contributed by IT-4F. It is observed that the EQE values are slightly higher in the short wavelength region than in the long wavelength region. This indicates the comparatively more efficient charge generation through the photo-induced electron transfer pathway than the hole transfer pathway. As is seen from the energy levels of the active layer materials, these polymers show small DE_{HOMO} less than the typical value of 0.30 eV for exciton dissociation. In comparison, the DE_{LUMO}s between the donor and acceptor are over 0.5 eV, which can supply enough driving force for exciton dissociation. Therefore, the EQE spectra exhibit slightly lower values in the acceptor region than in the donor region.[50] These results not only further con珞rm the values from the *J*–*V* curves, but also validate the effectiveness of the benzobis(thiazole) building block in the construction of excellent wide bandgap donor materials for NF-OSCs.

Table 2 Photovoltaic parameters of the OSCs under the illumination of AM 1.5G, 100 mW cm^{-2}

Polymers	V_{OC} [V]	J_{SC} [mA cm^{-2}]	J_{calc}[a] [mA cm^{-2}]	FF [%]	PCE[b] [%]	E_{loss}[c] [eV]
PBB-H	0.82	21.5	20.8	67.8	12.0 (11.9 ± 0.2)	0.72
PBB-F	0.92	22.4	21.3	71.1	14.7 (14.3 ± 0.3)	0.62
PBB-Cl	0.94	21.8	21.0	72.5	14.8 (14.5 ± 0.2)	0.60

[a] Calculated from EQE curves. [b] The average PCE values in the parentheses are calculated from 20 individual devices. [c] E_{loss} ¼ E_g — eV_{OC}.

To con珐rm the exciton dissociation behavior with the small E_{HOMO} offset, the exciton dissociation probability of the optimal devices was investigated. Fig. 4a shows the dependence of photocurrent density (J_{ph}) on effective voltage (V_{eff}) plots in double-logarithmic coordinates. J_{ph} is de珐ned as J_L—J_D, where J_L and J_D are the current densities under illumination and in the dark, respectively. V_{eff} is de珐ned as V_0 — V, where V_0 is the voltage at J_{ph} ¼ 0 and V is the applied voltage. For all three polymers, the J_{ph}s increased at low effective voltage and gradually reached a plateau with a saturation photocurrent density (J_{sat}) of about 22 mA cm^{-2}, indicating that the photogenerated free charges were swept out efficiently. The exciton dissociation probabilities (P_{diss} ¼ J_{ph}/J_{sat}) are calculated to be rv98% under short circuit conditions for all three devices, suggesting comparable and efficient charge generation and collection in the devices even with a small DE_{HOMO} of 0.06 eV for the PBB-Cl:IT-4F blend. Comparatively, the J_{ph}s are saturated at a lower V_{eff} for PBB-F and PBB-Cl (rv0.2 V) than for PBB-H (rv0.4 V), which indicates that charge collection would be more hindered by charge recombination in the PBB-H based device and would be correlated with a slightly lower FF value.

Charge recombination behavior is investigated using the light intensity (P_{light}) dependent J_{SC} and V_{OC} of solar cells. Under short circuit conditions, the photo-generated charges are mostly swept out of the devices and the bimolecular recombination of photo-induced carriers is usually negligible. The dependence of J_{SC} upon P_{light} (J_{SC} 珽 P_{light}^{a}) was examined and is shown in Fig. 4b. Exponential factors (a) of 0.96, 0.98 and 0.99 were measured for the devices based on PBB-H, PBB-F, and PBB-Cl, respectively, which indicates the comparatively more bimolecular recombination in the PBB-H based device. Under open circuit conditions, the current is zero and all photo-generated charges recombined within the device. Therefore, it is particularly sensitive to the recombination mechanism. The dependence of V_{OC} upon P_{light} is described by V_{OC} 珽 (nkT/q) ln(P_{light}), in which k is the Boltzmann constant, T is the temperature in Kelvin, and q is the elementary charge. The parameter n (usually $1 < n < 2$) re珠ects trap assisted charge recombination in the device. As shown in Fig. 4c, n ¼ 1.37, 1.21 and 1.24 were estimated for the devices based on PBB-H, PBB-F, and PBB-Cl, respectively, signifying more serious trap-assisted recombination in PBB-H based blends and comparably less recombination in the others. These results demonstrate that the introduction of halogen would reduce the recombination of charges generated in the devices, which would be responsible for the higher FF values of the devices based on PBB-F and PBB-Cl.

The hole mobilities (m_h) of the pristine and blend 珐lms were measured using the space-charge limited current (SCLC) method with the hole only devices (ITO/PEDOT:PSS/active layer/MoO_3/Al), and the results are shown in Fig. S6.† In the pristine 珐lm, the hole mobilities were determined to be 6.14×10^{-5}, 1.43×10^{-5} and 2.70×10^{-5} cm^2 V^{-1} s^{-1} for PBB-H, PBB-F and PBB-Cl, respectively. While in the blend 珐lms with IT-4F, PBB-H, PBB-F and PBB-Cl show increased hole mobility of 2.40×10^{-5}, 6.29×10^{-5} and 1.04×10^{-4} cm^2 V^{-1} s^{-1}, respectively. The higher mobilities of the halogenated polymer blends indicate better hole transport abilities which would be advantageous in achieving higher J_{SC} and FF values.

Film morphology analysis

The surface morphologies of the blend 珐lms were investigated by atomic force microscopy (AFM). As shown in Fig. 5a, a root-mean-square (RMS) roughness of 1.13, 0.93, and 1.24 nm is obtained for the blend 珐lms of PBB-H, PBB-F, and PBB-Cl, respectively. A smooth 珐lm roughness indicates good misci- bility between donor and acceptor materials, which is useful for efficient exciton dissociation. To further investigate the molec- ular packing and crystallinity behavior of these polymers, grazing incidence wide-angle X-ray diffraction (GIWAXS) measurement was performed for the pristine and blend 珐lms. The two-dimensional GIWAXS patterns and the corresponding in-plane (IP) and out-of-plane (OOP) line-cut pro珐les are shown in Fig. 5 and Fig. S7,† respectively. It is observed that the neat face-on orientation is dominant for all the pristine polymer
珐lms with distinct p–p stacking (010) and lamellar stacking (100) diffraction peaks in the out-of-plane and in-plane direction, respectively. The (010) and (100) peaks are generally located at about 0.25 and 1.7 Å^{-1}, corresponding to a lamellar stacking distance of approximately 24 Å and p–p stacking distance of approximately 3.6 Å. Comparatively, PBB-F exhibits a smaller p–p stacking distance of 3.59 Å than PBB-H and PBB-Cl (3.65 Å), which would be induced by the F incorporated intermolecular interaction. PBB-F and PBB-Cl show similar lamellar distances of 24.7 and 24.8 Å, which is slightly larger than that of PBB-H (24.3 Å). The full width half maximum (FWHM) of the (100) peaks of PBB-H, PBB-F, and PBB-Cl 珐lms is calculated to be 0.101, 0.075 and 0.070 Å^{-1}, corresponding to

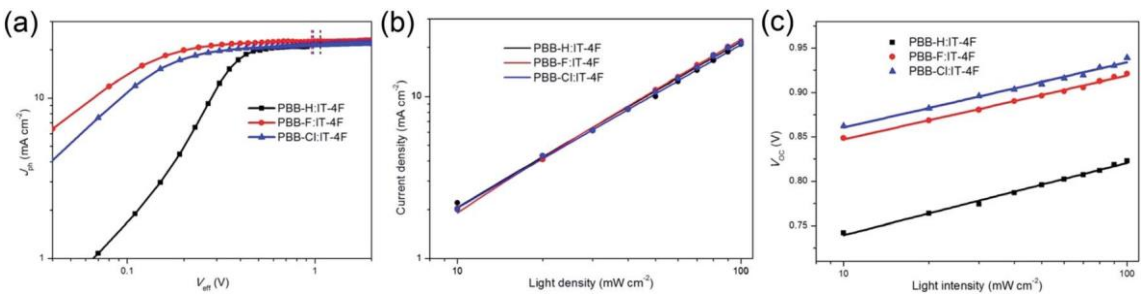

Fig. 4 (a) Photocurrent density (J_{ph}) *versus* effective voltage (V_{eff}) of the devices. Dependence of (b) J_{SC} and (c) V_{OC} on P_{light} of the devices.

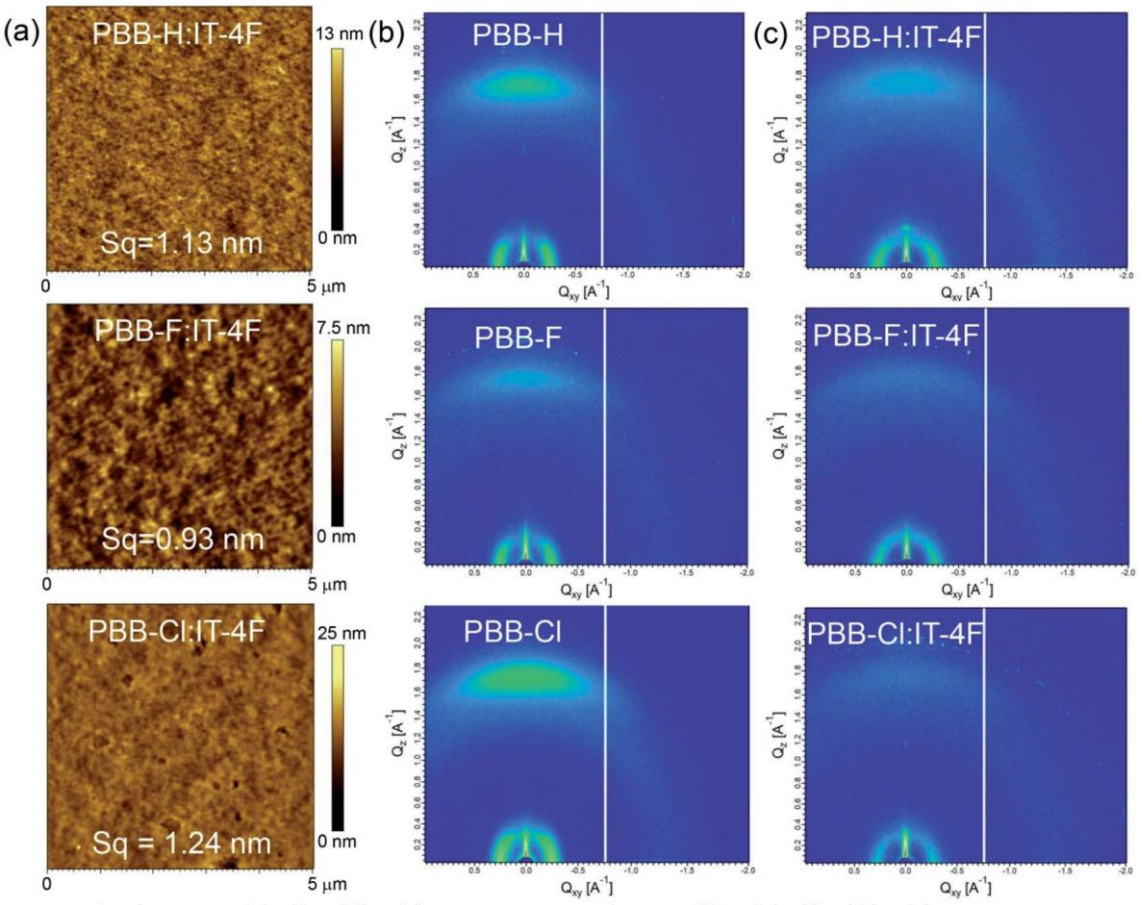

Fig. 5 AFM height images of the blend films (a). GIWAXS patterns of pristine (b) and the blend films (c).

a similar coherence length (L_C) of 6.2, 8.4 and 8.9 nm respectively, indicating more ordered crystal size and quality in the lamellar stacking direction for the F- and Cl-incorporated polymer 珡lms. Compared to that of the previously reported results for the polymer PBB-T,[39] the p–p stacking is slightly closer for these 2D-BBT based polymers, which would be induced by their better molecular planarity and extension of the conjugated backbone. It seems that the BBT-based polymers usually adopt a dominant face-on orientation, which might be induced by the centrosymmetric planar BBT structure and would be a unique feature of the BBT based polymers. The face-on orientation has been found to be helpful in reducing non-radiative recombination,[51] which would be responsible for high J_{SC}s and efficiencies achieved in the devices.

In the blend 珡lms of polymer:IT-4F, dominant face-on orientations are also observed just with a lower intensity. Compared to the pristine polymer 珡lms, the blend 珡lms show a similar p–p stacking distance of rv3.6 Å in the OOP direction, while the coherence lengths become decreased. The PBB-Cl:IT-4F blend 珡lm shows a larger L_C of 2.1 nm than the other two blend 珡lms (with L_Cs of 1.6 nm). This signi珡es the stronger p–p stacking interaction of PBB-Cl. Interestingly, the lamellar stacking distances are decreased to rv22.8 Å in the blend 珡lms compared to those of the corresponding pristine 珡lms, which could probably be induced by intermolecular interaction between the polymer and IT-4F. The blend 珡lms of PBB-F:IT-4F and PBB-Cl:IT-4F exhibit a larger L_C of 5.7 nm than the blend 珡lm of PBB-H:IT-4F (5.3 nm), which is coherent with the observation in pristine 珡lms. These results demonstrate that the dominant face-on orientation is preserved by the polymers in blend 珡lms, which is favorable for suppressing charge recombination and improving charge transport in the vertical direction of the substrate.[52] Introduction of F- and Cl-atoms can improve the crystallinity with increased coherence length, which would further improve charge mobilities and ameliorate the photovoltaic performance of the devices.

Conclusions

In summary, a series of polymers based on a 2D conjugated BBT unit was designed and synthesized for non-fullerene organic solar cells. Halogen atoms F and Cl were incorporated to modulate the energy levels and 珡lm morphology. The polymers exhibited high extinction coefficient, intense aggregation, and cascade energy level alignment. High power conversion efficiencies of 14.7% and 14.8% were achieved for PBB-F and PBB-Cl, respectively with IT-4F as the acceptor material in the photovoltaic devices. High J_{SC} values of over 21 mA cm^{-2} were

achieved for all three polymers, which could be attributed to their high extinction coefficient and favorable face-on orientation. Introduction of Cl atoms provides an open circuit voltage of 0.94 V, which is one of the highest values for devices with IT-4F as the acceptor. Well-balanced J_{SC} and V_{OC} values were eventually achieved through halogenation of the BBT-based polymer. The GIWAXS results indicate dominant face-on orientation for all three polymer 珡lms, which is valuable for charge transport in the vertical direction of the substrate and reducing charge recombination, thus achieving high J_{SC} and efficiencies. These results indicate that the polymers based on the 2D conjugated BBT unit would be a very promising candidate as a donor material for organic solar cells.

Conflicts of interest

There are no con珓icts to declare.

Acknowledgements

This work was supported by the National Key R&D Program of China (2016YFE0115000) and the Department of Science and Technology of Shandong Province (2019GGX102020). X. Bao also thanks the Youth Innovation Promotion Association CAS (2016194). The authors also thank the beamline BL16B1 of Shanghai Synchrotron Radiation Facility for providing the beam time and useful discussion.

Notes and references

1 P. Cheng, G. Li, X. Zhan and Y. Yang, *Nat. Photonics*, 2018, 12, 131.
2 C. H. Cui and Y. F. Li, *Energy Environ. Sci.*, 2019, 12, 3225.
3 L. Meng, Y. Zhang, X. Wan, C. Li, X. Zhang, Y. Wang, X. Ke, Z. Xiao, L. Ding, R. Xia, H.-L. Yip, Y. Cao and Y. Chen, *Science*, 2018, 361, 1094.
4 O. Inganaes, *Adv. Mater.*, 2018, 30, 1800388.
5 Y. Lin, J. Wang, Z.-G. Zhang, H. Bai, Y. Li, D. Zhu and X. Zhan, *Adv. Mater.*, 2015, 27, 1170.
6 J. Yuan, Y. Zhang, L. Zhou, G. Zhang, H.-L. Yip, T.-K. Lau, X. Lu, C. Zhu, H. Peng, P. A. Johnson, M. Leclerc, Y. Cao, J. Ulanski, Y. Li and Y. Zou, *Joule*, 2019, 3, 1140.
7 X. Xu, T. Yu, Z. Bi, W. Ma, Y. Li and Q. Peng, *Adv. Mater.*, 2018, 30, 1703973.
8 C. Sun, S. Qin, R. Wang, S. Chen, F. Pan, B. Qiu, Z. Shang, L. Meng, C. Zhang, M. Xiao, C. Yang and Y. Li, *J. Am. Chem. Soc.*, 2020, 142, 1465.
9 H. Yao, Y. Cui, D. Qian, C. S. Ponseca Jr, A. Honarfar, Y. Xu, J. Xin, Z. Chen, L. Hong, B. Gao, R. Yu, Y. Zu, W. Ma, P. Chabera, T. Pullerits, A. Yartsev, F. Gao and J. Hou, *J. Am. Chem. Soc.*, 2019, 141, 7743.
10 Y. Li, N. Zheng, L. Yu, S. Wen, C. Gao, M. Sun and R. Yang, *Adv. Mater.*, 2019, 31, 1807832.
11 S. F. Hoe珓er, T. Rath, N. Pastukhova, E. Pavlica, D. Scheunemann, S. Wilken, B. Kunert, R. Resel, M. Hobisch, S. Xiao, G. Bratina and G. Trimmel, *J. Mater. Chem. A*, 2018, 6, 9506.
12 Y. Wu, S. Schneider, C. Walter, A. H. Chowdhury, B. Bahrami, H.-C. Wu, Q. Qiao, M. F. Toney and Z. Bao, *J. Am. Chem. Soc.*, 2020, 142, 392.
13 J. Zhao, Y. Li, G. Yang, K. Jiang, H. Lin, H. Ade, W. Ma and H. Yan, *Nat. Energy*, 2016, 1, 15027.
14 H. Bin, L. Gao, Z.-G. Zhang, Y. Yang, Y. Zhang, C. Zhang, S. Chen, L. Xue, C. Yang, M. Xiao and Y. Li, *Nat. Commun.*, 2016, 7, 13651.
15 Z. Zheng, Q. Hu, S. Q. Zhang, D. Y. Zhang, J. Q. Wang, S. K. Xie, R. Wang, Y. P. Qin, W. N. Li, L. Hong, N. N. Liang, F. Liu, Y. Zhang, Z. X. Wei, Z. Y. Tang, T. P. Russell, J. H. Hou and H. Q. Zhou, *Adv. Mater.*, 2018, 30, 1801801.
16 S. Wang, Z. Li, X. Xu, M. Zhang, G. Zhang, Y. Li and Q. Peng, *J. Mater. Chem. A*, 2018, 6, 22503.
17 Z. He, C. Zhong, X. Huang, W.-Y. Wong, H. Wu, L. Chen, S. Su and Y. Cao, *Adv. Mater.*, 2011, 23, 4636.
18 Z. A. Page, Y. Liu, V. V. Duzhko, T. P. Russell and T. Emrick, *Science*, 2014, 346, 441.
19 Z. G. Zhang, B. Y. Qi, Z. W. Jin, D. Chi, Z. Qi, Y. F. Li and J. Z. Wang, *Energy Environ. Sci.*, 2014, 7, 1966.
20 J. Li, N. Wang, Y. Wang, Z. Liang, Y. Peng, C. Yang, X. Bao and Y. Xia, *Sol. Energy*, 2020, 196, 168.
21 G. Li, V. Shrotriya, J. S. Huang, Y. Yao, T. Moriarty, K. Emery and Y. Yang, *Nat. Mater.*, 2005, 4, 864.
22 M. Campoy-Quiles, T. Ferenczi, T. Agostinelli, P. G. Etchegoin, Y. Kim, T. D. Anthopoulos, P. N. Stavrinou, D. D. C. Bradley and J. Nelson, *Nat. Mater.*, 2008, 7, 158.
23 J. Li, Y. Wang, Z. Liang, J. Qin, M. Ren, J. Tong, C. Yang, X. Bao and Y. Xia, *J. Mater. Chem. C*, 2020, 8, 2483.
24 B. Fan, Z. Zeng, W. Zhong, L. Ying, D. Zhang, M. Li, F. Peng, N. Li, F. Huang and Y. Gao, *ACS Energy Lett.*, 2019, 4, 2466.
25 C. Sun, F. Pan, S. Chen, R. Wang, R. Sun, Z. Shang, B. Qiu, J. Min, M. Lv, L. Meng, C. Zhang, M. Xiao, C. Yang and Y. Li, *Adv. Mater.*, 2019, 31, 1905480.
26 Z. Zhou, W. Liu, G. Zhou, M. Zhang, D. Qian, J. Zhang, S. Chen, S. Xu, C. Yang, F. Gao, H. Zhu, F. Liu and X. Zhu, *Adv. Mater.*, 2020, 32, 1906324.
27 S. Liu, J. Yuan, W. Deng, M. Luo, Y. Xie, Q. Liang, Y. Zou, Z. He, H. Wu and Y. Cao, *Nat. Photonics*, 2020, 14, 300.
28 T. Kirchartz and U. Rau, *Adv. Energy Mater.*, 2018, 8, 1703385.
29 D. Qian, Z. Zheng, H. Yao, W. Tress, T. R. Hopper, S. Chen, S. Li, J. Liu, S. Chen, J. Zhang, X.-K. Liu, B. Gao, L. Ouyang, Y. Jin, G. Pozina, I. A. Buyanova, W. M. Chen, O. Inganas, V. Coropceanu, J.-L. Bredas, H. Yan, J. Hou, F. Zhang, A. A. Bakulin and F. Gao, *Nat. Mater.*, 2018, 17, 703.
30 G. Zhang, J. Zhao, P. C. Y. Chow, K. Jiang, J. Zhang, Z. Zhu, J. Zhang, F. Huang and H. Yan, *Chem. Rev.*, 2018, 118, 3447.
31 S. Dai, F. Zhao, Q. Zhang, T.-K. Lau, T. Li, K. Liu, Q. Ling, C. Wang, X. Lu, W. You and X. Zhan, *J. Am. Chem. Soc.*, 2017, 139, 1336.
32 R. Wang, J. Yuan, G. Han, T. Huang, W. Huang, J. Xue, H.-C. Wang, C. Zhang, C. Zhu, P. Cheng, D. Meng, Y. Yi, K.-H. Wei, Y. Zou and Y. Yang, *Adv. Mater.*, 2019, 31, 1904215.

33 S. Zhang, Y. Qin, J. Zhu and J. Hou, *Adv. Mater.*, 2018, 30, 1800868.
34 A. Tang, W. Song, B. Xiao, J. Guo, J. Min, Z. Ge, J. Zhang, Z. Wei and E. Zhou, *Chem. Mater.*, 2019, 31, 3941.
35 A. Tang, Q. Zhang, M. Du, G. Li, Y. Geng, J. Zhang, Z. Wei, X. Sun and E. Zhou, *Macromolecules*, 2019, 52, 6227.
36 H. Chen, Z. Hu, H. Wang, L. Liu, P. Chao, J. Qu, W. Chen, A. Liu and F. He, *Joule*, 2018, 2, 1623.
37 P. Chao, N. Johner, X. Zhong, H. Meng and F. He, *J. Energy Chem.*, 2019, 39, 208.
38 D. Mo, H. Chen, J. Zhou, N. Tang, L. Han, Y. Zhu, P. Chao, H. Lai, Z. Xie and F. He, *J. Mater. Chem. A*, 2020, 8, 8903.
39 Y. Lin, H. Fan, Y. Li and X. Zhan, *Adv. Mater.*, 2012, 24, 3087.
40 I. Osaka, K. Takimiya and R. D. McCullough, *Adv. Mater.*, 2010, 22, 4993.
41 A. Bhuwalka, M. D. Ewan, M. Elshobaki, J. F. Mike, B. Tlach, S. Chaudhary and M. Jeffries-El, *J. Polym. Sci., Part A: Polym. Chem.*, 2016, 54, 316.
42 S. Wen, Y. Li, T. Rath, Y. Li, Y. Wu, X. Bao, L. Han, H. Ehmann, G. Trimmel, Y. Zhang and R. Yang, *Chem. Mater.*, 2019, 31, 919.
43 P. Chao, H. Wang, S. Qu, D. Mo, H. Meng, W. Chen and F. He, *Macromolecules*, 2017, 50, 9617.
44 S. Zhang, J. Zhang, M. Abdelsamie, Q. Shi, Y. Zhang, T. C. Parker, E. V. Jucov, T. V. Timofeeva, A. Arnassian, G. C. Bazan, S. B. Blakey, S. Barlow and S. R. Marder, *Chem. Mater.*, 2017, 29, 7880.
45 L. Huo, S. Zhang, X. Guo, F. Xu, Y. Li and J. Hou, *Angew. Chem., Int. Ed.*, 2011, 50, 9697.
46 X. Bao, Y. Zhang, J. Wang, D. Zhu, C. Yang, Y. Li, C. Yang, J. Xu and R. Yang, *Chem. Mater.*, 2017, 29, 6766.
47 Z.-G. Zhang, B. Qi, Z. Jin, D. Chi, Z. Qi, Y. Li and J. Wang, *Energy Environ. Sci.*, 2014, 7, 1966.
48 Y. Cui, H. Yao, L. Hong, T. Zhang, Y. Xu, K. Xian, B. Gao, J. Qin, J. Zhang, Z. Wei and J. Hou, *Adv. Mater.*, 2019, 31, 1808356.
49 W. Zhao, S. Li, H. Yao, S. Zhang, Y. Zhang, B. Yang and J. Hou, *J. Am. Chem. Soc.*, 2017, 139, 7148.
50 Y. Xie, W. Wang, W. Huang, F. Lin, T. Li, S. Liu, X. Zhan, Y. Liang, C. Gao, H. Wu and Y. Cao, *Energy Environ. Sci.*, 2019, 12, 3556.
51 N. A. Ran, S. Roland, J. A. Love, V. Savikhin, C. J. Takacs, Y.-T. Fu, H. Li, V. Coropceanu, X. Liu, J.-L. Bredas, G. C. Bazan, M. F. Toney, D. Neher and N. Thuc-Quyen, *Nat. Commun.*, 2017, 8, 79.
52 S. Shoaee, M. Stolterfoht and D. Neher, *Adv. Energy Mater.*, 2018, 8, 1703355.

